

Generalized synchronization in mutually coupled oscillators and complex networks

Olga I. Moskalenko^{1,*}, Alexey A. Koronovskii^{1,†}, Alexander E. Hramov^{1,‡} and Stefano Boccaletti²

¹ Faculty of Nonlinear Processes, Saratov State University, Astrakhanskaya, 83, Saratov, 410012, Russia
Saratov State Technical University, Politehnicheskaya, 77, Saratov, 410054, Russia

² CNR — Istituto dei Sistemi Complessi Via Madonna del Piano, 10 50019 Sesto Fiorentino (FI), Italy

(Dated: September 7, 2018)

We introduce a novel concept of generalized synchronization, able to encompass the setting of collective synchronized behavior for mutually coupled systems and networking systems featuring complex topologies in their connections. The onset of the synchronous regime is confirmed by the dependence of the system's Lyapunov exponents on the coupling parameter. The presence of a generalized synchronization regime is verified by means of the nearest neighbor method.

PACS numbers: 05.45.Tp, 05.45.Vx, 05.45.Xt

Keywords: chaotic oscillators, generalized synchronization, mutual coupling, Lyapunov exponents, network

INTRODUCTION

Synchronization of chaotic systems is a subject widely studied in recent years, having both theoretical and applied significance [1]. Of a particular interest is the intricate phenomenon of generalized synchronization (GS), originally introduced as an emerging collective motion of unidirectionally coupled chaotic oscillators [2, 3]. GS has been, indeed, observed in numerous systems, both numerically [4–6] and experimentally [7–9], and its main features [5, 10] have suggested many possible applications [11–13].

The very same concept of GS has been introduced initially in the case of two unidirectionally coupled oscillators, the drive (or master) $\mathbf{x}(t)$ system and the response (or slave) $\mathbf{u}(t)$ one. GS means the presence of a time independent functional relation $\mathbf{F}[\cdot]$ between the master and slave system states, after a suitable transient time interval is elapsed [14], i.e.

$$\mathbf{u}(t) = \mathbf{F}[\mathbf{x}(t)]. \quad (1)$$

In this Paper, we report on the extension of the concept of GS for both oscillators with a bidirectional coupling, and for complex networks' architectures. It is, indeed, evident that Eq. (1) needs to be extended for reflecting the fact that a mutual interaction exists between the systems under study. The traditional definition of GS in the form of (1) introduced for the unidirectionally coupled chaotic oscillators is based on the fact that the drive system state $\mathbf{x}(t)$ does not depend on the state of the response system $\mathbf{u}(t)$. Hence, for the GS regime Eq. (1) may be applied at every moment of time t . In the case of the mutual type of coupling between systems the situation is radically different, since the interacting oscillators are equivalent from the point of view of the coupling, and the evolution of the first system is determined not only by

the vector $\mathbf{x}(t)$, but also by the the state of the second system $\mathbf{u}(t)$, and vice versa. Therefore, in the general case the functional relation between states of the mutually coupled systems can not be written in the explicit form (1), and, as a consequence, the implicit functional relation must be used. To take into account the common action of the systems on each other, we here propose to modify Eq. (1) for two chaotic oscillators as

$$\mathbf{F}[\mathbf{x}(t), \mathbf{u}(t)] = 0. \quad (2)$$

Note, Eq. (2) may be used to inspect both the unidirectional and the bidirectional types of the coupling (as well as any coupling with arbitrary asymmetry between the systems). Furthermore, Eq. (1) can be considered as a special case of (2).

For a generic ensemble of N elements Eq. (3) can be rewritten as following

$$\mathbf{F}[\mathbf{x}_1(t), \mathbf{x}_2(t), \dots, \mathbf{x}_i(t), \dots, \mathbf{x}_N(t)] = 0, \quad (3)$$

where $\mathbf{x}_i(t)$ is the vector state of the i -th element of the network. In other words, we assume that the generalized synchronization regime implies the presence of a functional relation between the system states, as before, but this relation takes the implicit form (3) instead of (1), i.e. it implies the arousal of a generic manifold in phase-space wherein the overall trajectory is lying during its time evolution.

I. GENERALIZED SYNCHRONIZATION, LYAPUNOV EXPONENTS AND THE NEAREST NEIGHBOR METHOD

For the unidirectionally coupled oscillators the Lyapunov exponents calculation is known to allow to detect the GS boundary more precisely in comparison with the nearest neighbor method, whereas the last one gives mostly only the qualitative confirmation of the GS regime presence. Therefore, we propose to use the Lyapunov exponents to detect the GS regime in the mutually coupled systems. As far as the nearest neighbor method is

*Electronic address: o.i.moskalenko@gmail.com

†Electronic address: alkor@nonlin.sgu.ru

‡Electronic address: aeh@nonlin.sgu.ru

concerned, we use it for the verification of the obtained results.

If the dimensions of the drive and response systems are N_d and N_r respectively, the behavior of the unidirectionally coupled oscillators is characterized by the Lyapunov exponent spectrum $\lambda_1 \geq \lambda_2 \geq \dots \geq \lambda_{N_d+N_r}$. Due to the independence of the drive system dynamics on the behavior of the response one, the Lyapunov exponent spectrum may be divided into two parts [15, 16]: LEs of the drive system $\lambda_1^d \geq \dots \geq \lambda_{N_d}^d$ and LEs of the response one $\lambda_1^r \geq \dots \geq \lambda_{N_r}^r$. For the GS detection in the unidirectionally coupled chaotic oscillators the Lyapunov exponents calculated for the response system play the key role (since the behavior of the response depends on the drive, these Lyapunov exponents are called conditional). With the increase of the coupling strength the largest conditional Lyapunov exponent λ_1^r becomes negative at the onset of the GS regime [17]. Thus, the negativity of the largest conditional Lyapunov exponent

$$\lambda_1^r < 0 \quad (4)$$

is considered as a criterion of the GS presence in the unidirectionally coupled dynamical systems [3, 16].

Since in the case of the mutual coupling the spectrum of Lyapunov exponents cannot be divided into two parts corresponding to the drive and response systems, condition (4) must also be modified. Notice that, here, the dimension of each element is assumed to be $N_d = 3$, but this analytical study may be extended easily to the other systems with arbitrary dimensions N_d .

As it has already been mentioned, in the neighborhood of any moment of time t [35] Eq. (2) may be considered as the definition of the implicit functional relation between system states, and, therefore, according to the implicit-function theorem [18], locally, the implicit definition of the functional relation between system states may be used, i.e., $\mathbf{x}(t) = \tilde{\mathbf{F}}[\mathbf{u}(t)]$ or $\mathbf{u}(t) = \tilde{\mathbf{F}}[\mathbf{x}(t)]$. Let us assume without the lack of the generality that for $t^* - \delta < t < t^* + \delta$ (where δ is infinitely small) the implicit functional relation

$$\mathbf{x}(t^*) = \tilde{\mathbf{F}}[\mathbf{u}(t^*)] \quad (5)$$

is defined with the help of Eq. (2). In this case, locally, in the given range $t^* - \delta < t < t^* + \delta$, we deal with the already studied case of Eq. (1). Eq. (5) means that (under assumption $N_d = 3$ made above) the following local Lyapunov exponents characterize the dynamics of the systems: $\lambda_1^u > 0$, $\lambda_2^u = 0$, $\lambda_3^u < 0$, $\lambda_{1,2,3}^x < 0$. In other words, in the selected area of the $6D$ phase-space the manifold corresponding to the GS regime is characterized by one unstable direction \mathbf{e}^u and one direction with the neutral stability \mathbf{e}^0 lying inside this manifold, whereas all other directions are stable. These directions correspond to one positive, one zero and four negative Lyapunov exponents. The same statement is also correct for the other moments of time t^* , although the implicit functional relation may take form $\mathbf{u}(t^*) = \tilde{\mathbf{F}}[\mathbf{x}(t^*)]$ instead of (5). So, one can come to conclusion that in the

case of the mutual type of coupling the manifold corresponding to the GS regime at every moment of time is characterized by one unstable direction, one direction with the neutral stability and four stable directions. So, having calculated the spectrum of Lyapunov exponents for two bidirectionally coupled chaotic oscillators one obtains that the GS regime in this case produces one positive, one zero and four negative Lyapunov exponents. Since in the case of the mutual coupling one cannot pick out the conditional Lyapunov exponents, the criterion of the GS regime should be written in the form

$$\lambda_3 < 0, \quad (6)$$

whereas $\lambda_1 > 0$, $\lambda_2 = 0$.

Having extended this theoretical consideration to the complex networks (where the implicit form of the functional relation is given by (3)) one can obtain that condition (6) remains also correct for the GS regime existence in these networks.

To validate the presence of the generalized synchronization regime, in parallel with the calculation of the spectrum of Lyapunov exponents, one can also make use of the nearest neighbor method [14, 19]. The main idea of this technique consists in the fact that the presence of the functional relation between the interacting system states means that all close states (“origins”) in the phase subspace of a given system $\mathbf{x}(t)$ should correspond to close states (“images”) in the phase sub-space of the other one $\mathbf{u}(t)$ (see [14] for details). For mutually coupled oscillators the inverse statement must be also correct, i.e. all close states in the phase sub-space of the second system $\mathbf{u}(t)$ must correspond to close states of the first one $\mathbf{x}(t)$.

As a numerical indicator of the existence of a functional relationship between the interacting systems, the mean distance between images $\mathbf{u}^{k, kn}$ of nearest neighbors $\mathbf{x}^{k, kn}$ normalized by the average distance δ of randomly chosen states of the first system, i.e.

$$d = \frac{1}{M\delta} \sum_{k=0}^{M-1} \|\mathbf{u}^k - \mathbf{u}^{kn}\|, \quad (7)$$

can be calculated (here M is the number of the points chosen randomly) [19]. This characteristic allows to reveal the qualitative changes in the synchronous/asynchronous behavior of the coupled systems. When the coupling between systems is very small and oscillators show the asynchronous dynamics the value of this measure is $d \sim 1$. The phase synchronization regime causes the sharp decrease of the value d but it differs from zero sufficiently, as before, whereas deep inside the generalized synchronization region d tends to be zero due to the presence of the functional relation between states of the interacting systems. In the vicinity of the GS boundary (both inside and outside the GS area) the value of d -quantity decreases slowly to zero value, with the onset of the generalized synchronization regime corresponding approximately to the middle of this transition interval.

Unfortunately, the nearest neighbor method does not allow to detect precisely the boundary points of the GS regime, but it allows to confirm the presence of GS and to estimate the location of the GS boundary.

To illustrate the proposed approach, we use several cases, and start our considerations from two mutually coupled Rössler oscillators

$$\begin{aligned} \dot{x}_{1,2} &= -\omega_{1,2}y_{1,2} - z_{1,2} + \varepsilon(x_{2,1} - x_{1,2}), \\ \dot{y}_{1,2} &= \omega_{1,2}x_{1,2} + ay_{1,2}, \\ \dot{z}_{1,2} &= p + z_{1,2}(x_{1,2} - c), \end{aligned} \quad (8)$$

where $\mathbf{x}_{1,2}(t) = (x_{1,2}, y_{1,2}, z_{1,2})^T$ are the vector-states of the interacting systems, ε is a coupling parameter. The control parameter values have been selected by analogy with our previous works [20–22] as $a = 0.15$, $p = 0.2$, $c = 10$. The parameter $\omega_{1,2}$ defines the natural frequency of oscillations, with $\omega_1 = 0.99$ and $\omega_2 = 0.95$ being fixed.

The behavior of the four largest Lyapunov exponents for the considered case is shown in Fig. 1, *a* and the dependence of the quantitative measure (7) on the coupling parameter strength ε is given in Fig. 1, *b*. One can see that at $\varepsilon_{LE} \approx 0.106$ the second Lyapunov exponent λ_2 passes through zero and becomes negative. Therefore, the generalized synchronization regime is expected to be observed above the critical value ε_{LE} . As far as the quantitative measure (7) is concerned, the curve $d(\varepsilon)$ decreases monotonically when the coupling parameter value increases. The $(\varepsilon; d)$ -plane can be divided into 4 parts: I – $\varepsilon \in [0; 0.04)$, the d -characteristic decreases very sharply indicating the transition from the asynchronous motion to the phase synchronization regime at $\varepsilon_{PS} = 0.04$; II – $\varepsilon \in [0.04; 0.09)$, d is not practically changed being the evidence of the phase synchronized motion; III – $\varepsilon \in [0.09; 0.12)$, the d -characteristic decreases slowly indicating the occurrence of the GS regime; IV – $\varepsilon > 0.12$, $d \approx 0$. Note, the bifurcation point $\varepsilon_{LE} \approx 0.106$ (where the second Lyapunov exponent λ_2 crosses the zero value and becomes negative) corresponds exactly to the middle of the transition interval III where d -characteristic decreases slowly to zero value. Later, at $\varepsilon_{LS} \approx 0.169$ the lag synchronization (LS) regime takes place.

In Fig. 1, *c-j* the phase portraits of the interacting Rössler systems (8) are shown for the different values of the coupling strength ε . In the phase portraits of the first system $\mathbf{x}(t)$ (Fig. 1, *c, e, g, i*) three randomly chosen points \mathbf{x}^k with its nearest neighbors \mathbf{x}^{kn} are shown. Figures 1, *d, f, h, j* illustrate the corresponding states $\mathbf{u}^{k, kn}$ in the phase sub-space of the second system $\mathbf{u}(t)$.

One can see easily that for the small values of the coupling parameter ($\varepsilon = 0.01$) all points of the second system are distributed randomly throughout the whole attractor (Fig. 1, *d*). When the coupling parameter value increases the points become to be concentrated in a limited portion of attractor, with the radius of the distribution area decreasing (compare Fig. 1, *f, h*). For $\varepsilon > \varepsilon_{LE}$ all states of the second system corresponding to the nearest states of the first oscillator are also nearest, and vice

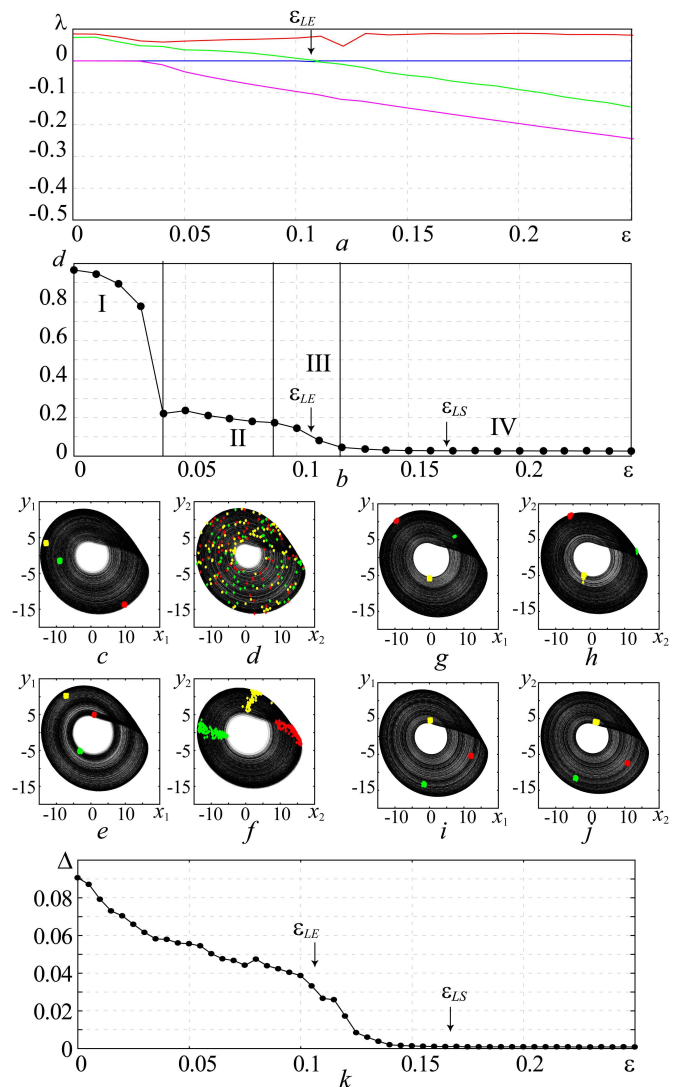


FIG. 1: (Color online) (a) The dependencies of the four largest Lyapunov exponents on the coupling strength ε for (8). (b) The quantitative measure d (7) versus the coupling parameter strength ε . The critical values of the coupling parameter $\varepsilon_{LE} = 0.106$ and $\varepsilon_{LS} = 0.169$ are marked by arrows. (c–j) The phase portraits of Rössler oscillators for the different values of the coupling parameter: (c–d) $\varepsilon = 0.01$ (the asynchronous state); (e–f) $\varepsilon = 0.05$ (the PS regime); (g–h) $\varepsilon = 0.12$ (the GS regime); (i–j) $\varepsilon = 0.18$ (the LS regime). Figures (c, e, g, i) show the chaotic attractor of the first system $\mathbf{x}(t)$ with three randomly chosen points \mathbf{x}^k and its nearest neighbors \mathbf{x}^{kn} . Figures (d, f, h, j) illustrate the corresponding states $\mathbf{u}^{k, kn}$ in the phase sub-space of the second system $\mathbf{u}(t)$. (k) The dependence of the mean distance Δ between shifted states of the interacted systems (8)

versa (Fig. 1, *g, h* and Fig. 1, *i, j*), that proves the occurrence of GS. Note also the difference between GS and LS which consists in the fact that in the LS regime the representation points corresponding to the nearest neighbors are practically in the same part of chaotic attractor (Fig. 1, *i, j*) whereas in the GS regime they can be located

in the slightly different regions (Fig. 1, *g,h*). The additional evidence of the fact that the GS and LS regimes differ from each other is the behavior of the mean distance Δ between the interacted system states shifted in time on the coupling parameter value. Such dependence is shown in Fig. 1, *k*. It is clearly seen that in the LS regime $\Delta \approx 0$ whereas in the GS regime it is a positive one.

II. GS IN MUTUALLY COUPLED SPATIALLY EXTENDED SYSTEMS

The very same results have also been obtained for two mutually coupled Pierce diodes being the classical models of beam-plasma systems, demonstrating the complex spatio-temporal oscillations including the chaotic ones [23, 24]. The dynamics of Pierce diodes (in the fluid electronic approximation) is described by the self-consistent system of dimensionless Poisson, continuity and motion equations [25]:

$$\begin{aligned} \frac{\partial^2 \varphi_{1,2}}{\partial x^2} &= -(\alpha_{1,2})^2 (\rho_{1,2} - 1), \\ \frac{\partial \rho_{1,2}}{\partial t} &= -\frac{\partial(\rho_{1,2} v_{1,2})}{\partial x}, \\ \frac{\partial v_{1,2}}{\partial t} &= -v_{1,2} \frac{\partial v_{1,2}}{\partial x} + \frac{\partial \varphi_{1,2}}{\partial x}, \end{aligned} \quad (9)$$

with the boundary conditions

$$v_{1,2}(0, t) = 1, \quad \rho_{1,2}(0, t) = 1, \quad \varphi_{1,2}(0, t) = 0, \quad (10)$$

where $\varphi_{1,2}(x, t)$ is the dimensionless potential of the electric field, $\rho_{1,2}(x, t)$ and $v_{1,2}(x, t)$ are the dimensionless density and velocity of the electron beam ($0 \leq x \leq 1$), the indexes “1” and “2” correspond to the first and second coupled beam-plasma systems, respectively, $\alpha_1 = 2.858\pi$, $\alpha_2 = 2.860\pi$ are the control parameters. The bidirectional coupling between considered Pierce diodes is realized by the modification of the boundary conditions on the right boundary of the systems, in the same way as it has been done in [26, 27]

$$\varphi_{1,2}(1, t) = \varepsilon(\rho_{1,2}(x=1, t) - \rho_{2,1}(x=1, t)), \quad (11)$$

where ε is a dimensionless coupling parameter.

Continuity and motion equations of (9) are integrated numerically with the help of the one-step explicit two-level scheme with upstream differences and the Poisson equation is solved by the method of the error vector propagation [28]. The time and space integration steps have been taken as $\Delta t = 0.003$ and $\Delta x = 0.005$, respectively.

For the GS regime detection the nearest neighbor method and calculation of the spectrum of Lyapunov exponents have also been used. In Fig. 2, *a* the dependencies of four largest Lyapunov exponents on the coupling parameter ε are shown. For computation of the spectrum of spatial Lyapunov exponents the method proposed in [29] has been used. It is clearly seen that as in the case of

mutually coupled Rössler systems two Lyapunov exponents do not practically depend on the coupling parameter ε , i.e. one Lyapunov exponent λ_1 is always positive (except the windows of periodicity) whereas the second one λ_3 remains zero. At the same time, two Lyapunov exponents (initially positive λ_2 and initially zero λ_4) depend on the coupling parameter and pass in the field of the negative values with the coupling parameter value increasing. One can assume, that as in the case of mutually coupled Rössler systems the transition of the positive Lyapunov exponent λ_2 in the field of the negative values (for $\varepsilon = \varepsilon_c = 0.078$) is connected with the generalized synchronization regime onset in mutually coupled beam-plasma systems.

To confirm the assumption made above the nearest neighbor method has been used. To characterize the degree of closeness of the interacted system states quantitatively the measure d defined by (7) has also been computed. As the interacted system states vectors $\mathbf{u}_{1,2}(x, t) = (\rho_{1,2}, v_{1,2}, \varphi_{1,2})^T$ have been used, whose norm $\|\cdot\|$ has been calculated as

$$\|\mathbf{u}\| = \sqrt{\int_0^L \rho dx + \int_0^L \varphi dx + \int_0^L v dx}. \quad (12)$$

In Fig. 2, *b* the dependence of the quantitative measure d on the coupling parameter ε is shown. It is clearly seen that d -characteristics decreases monotonically from one to zero with ε value increasing. At that, ε_c is approximately in the middle of the falling field $\varepsilon \in [0.04; 0.12]$, that indicates the generalized synchronization regime presence. It should be noted that generalized synchronization does not coincide with the complete synchronization regime in this case. For the control parameter values mentioned above it is realized for $\varepsilon \approx 0.17$.

Additional evidence of the presence of generalized synchronization regime in two mutually coupled beam plasma systems is the behavior of the nearest neighbors in the phase space of interacted systems. In Fig. 2, *c-h* the reconstructed attractors of interacted Pierce diodes on $(\rho_{1,2}(x=0.2, t), \rho_{1,2}(x=0.6, t))$ -plane for different values of the coupling parameter ε are shown. On attractors of the first system (Fig. 2, *c,e,g*) three randomly chosen points and its nearest neighbors are also indicated. Fig. 2, *d,f,h* illustrates the corresponding states in the phase space of the second system.

It is clearly seen that as in the case of Rössler systems for small values of the coupling parameter ($\varepsilon = 0.002$) all points in the phase space of the second system are distributed randomly over all attractor (see Fig. 2, *d*). With the coupling parameter value increasing the points begin grouping in the limited range of attractor that corresponds to the phase synchronization regime onset, with the radius of such field being decreased (compare Fig. 2, *f,h*). For $\varepsilon > \varepsilon_{LE}$ all states of the second beam-plasma system corresponding to the nearest neighbors of the first Pierce diode are also nearest and vice versa (Fig. 2, *g,h*), that is the evidence of the generalized synchronization regime presence.

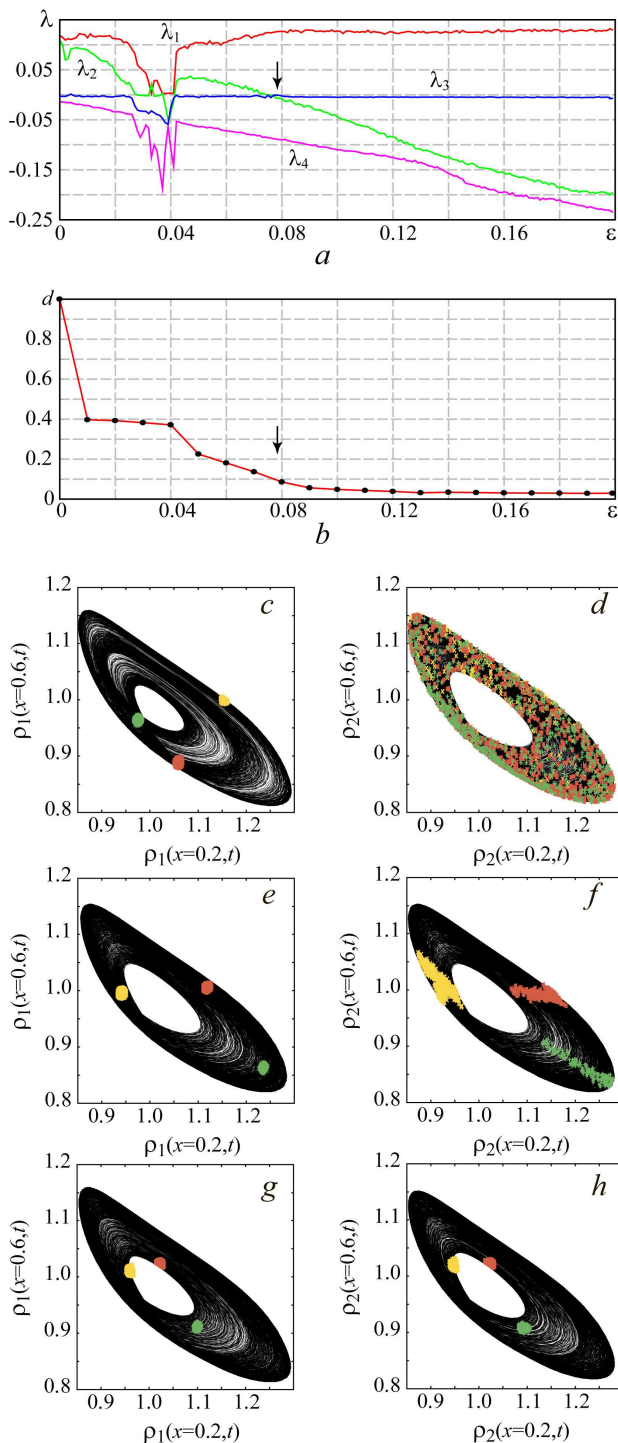


FIG. 2: (Color online) (a) The dependencies of the four largest Lyapunov exponents on the coupling strength ϵ for (9). (b) The quantitative measure d (7) versus the coupling parameter strength ϵ . The critical value of the coupling parameter $\epsilon_{LE} = 0.078$ corresponding to the zero-cross of the positive Lyapunov exponent is marked by arrow. (c-h) The reconstructed attractors of two mutually coupled Pierce diodes on $(\rho_{1,2}(x = 0.2, t), \rho_{1,2}(x = 0.6, t))$ -plane for the different values of the coupling parameter: (c,d) $\epsilon = 0.002$ (the asynchronous state), (e,f) $\epsilon = 0.05$ (the PS regime), (g,h) $\epsilon = 0.10$ (the GS regime). Figures (c,e,g) show the reconstructed attractor of the first Pierce diode with three randomly chosen points and its nearest neighbors. Figures (d,f,h) illustrate the corresponding states in the phase sub-space of the second Pierce diode

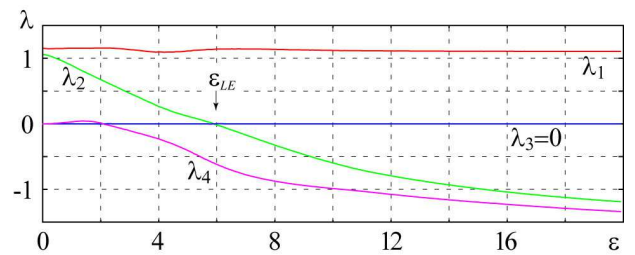


FIG. 3: (Color online) The dependencies of the four largest Lyapunov exponents on the coupling strength ϵ

So, on the basis of consideration carried out one can conclude that in both cases considered above, the onset of the GS regime is connected with the sign change of the initially positive Lyapunov exponent λ_2 in the same way as for two unidirectional oscillators [17]. As well as in the case of the chaotic oscillators coupled unidirectionally, for the systems with the bidirectional coupling the onset of the GS regime ϵ_{LE} precedes the boundary of lag or complete synchronization ϵ_{LS} .

III. GS IN MUTUALLY COUPLED LORENZ OSCILLATORS

To prove the made decisions conclusively, in this Section of the paper we consider another example of the oscillators coupled mutually, namely, two Lorenz systems

$$\begin{aligned} \dot{x}_{1,2} &= \sigma(y_{1,2} - x_{1,2}) + \varepsilon(x_{2,1} - x_{1,2}), \\ \dot{y}_{1,2} &= r_{1,2}x_{1,2} - y_{1,2} - x_{1,2}z_{1,2}, \\ \dot{z}_{1,2} &= -bz_{1,2} + x_{1,2}y_{1,2}. \end{aligned} \quad (13)$$

where $\mathbf{x}_{1,2}(t) = (x_{1,2}, y_{1,2}, z_{1,2})^T$ are the vector-states of the interacting systems, ε is a coupling parameter, $\sigma = 10.0$, $b = 8/3$, $r_1 = 40.0$ and $r_2 = 35.0$. Due to the bistable type of the chaotic attractor of the Lorenz oscillator there are certain particularities of the GS regime which do not take place in the systems with the Rössler-like chaotic attractor.

According to the decision made in Sec. I-II, the onset of the GS regime is connected with the sign change of the initially positive Lyapunov exponent λ_2 at $\epsilon_{LE} \approx 6.0$ (Fig. 3). To prove this statement for two mutually coupled Lorenz systems (13) we have used the nearest neighbor method again both below (Fig. 4, a,b) and above (Fig. 4, c,d) the critical point ϵ_{LE} . For this purpose the reference point \mathbf{x}^k and its nearest neighbors \mathbf{x}^{kn} have been selected in the phase space of the first Lorenz system (Fig. 4, a,c) and the corresponding to them points $\mathbf{u}^{k,kn}$ have been found in the phase space of the second Lorenz oscillator (Fig. 4, b,d). For $\epsilon > \epsilon_{LE}$ the existence of the GS regime is evidenced by the fact that all states of the second Lorenz system corresponding to the nearest states of the first oscillator are also nearest (Fig. 4, d). Alternatively, below the threshold ϵ the points of the sec-

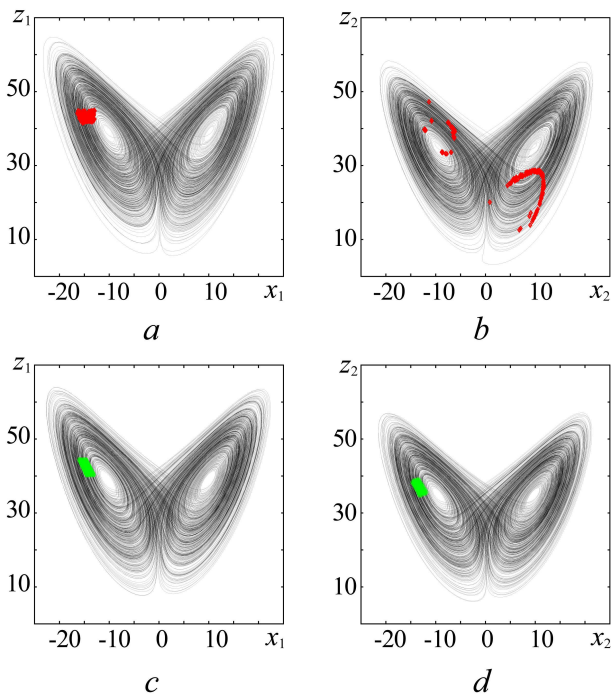


FIG. 4: (Color online) The phase portraits of two mutually coupled Lorenz oscillators (13) for $\varepsilon = 5.7$ (*a,b*) and $\varepsilon = 6.1$ (*c,d*). Figures (*a,c*) show the chaotic attractor of the first system $\mathbf{x}(t)$ with the reference point \mathbf{x}^k and its nearest neighbors \mathbf{x}^{kn} . Figures (*b,d*) illustrate the corresponding to them states $\mathbf{u}^{k,kn}$ in the phase space of the second system $\mathbf{u}(t)$

ond system are located on the both sheets of the chaotic attractor (Fig. 4, *b*) that indicates the break of GS.

Again, as well as for two mutually coupled Rössler systems (8) and Pierce diodes (9), the onset of the GS regime is shown to be connected with the sign change of the initially positive Lyapunov exponent λ_2 taking place when the coupling strength ε grows.

At the same time, in the dynamics of mutually coupled Lorenz oscillators (13) there are certain particularities connected with the occurrence of GS caused by the bistable type of the chaotic attractor of the system under study [36]. One can see easily that in the case under consideration the coupling strength value corresponding to the onset of GS is larger sufficiently than the analogous value for two mutually coupled Rössler systems (8) and Pierce diodes (9). Owing to the great coupling strength value, in the vicinity of the GS onset (below the bifurcation point ε_{LE}) two interacting Lorenz systems are greatly synchronized with each other almost all time except for the short time intervals when the representation point of one of the coupled oscillators remains in the one sheet of the chaotic attractor whereas the representation point of the second oscillator jumps to another sheet (see Fig. 5). After such a short jump both phase trajectories approach each other, and the oscillators start showing synchronous dynamics again. It is the short-time

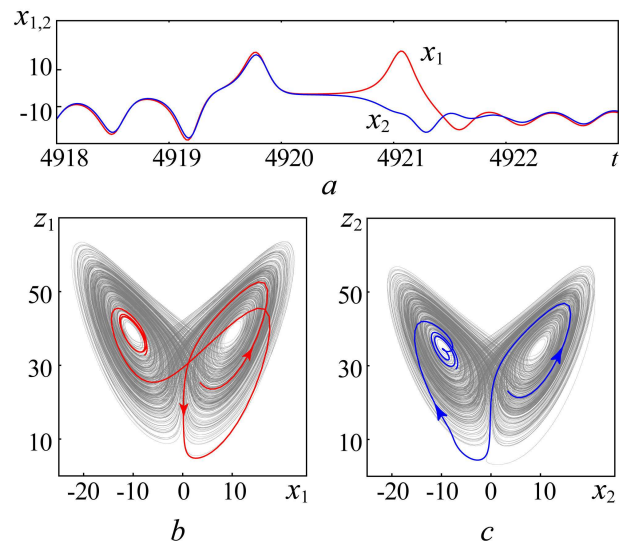


FIG. 5: (Color online) (*a*) The fragment of the time series of two mutually coupled Lorenz oscillators (13) corresponding to the short-term period of the phase trajectory divergence. (*b*) The phase portraits of Lorenz systems and the phase trajectories corresponding to the time interval shown in Fig. 5, *a*. The coupling strength $\varepsilon = 5.7$, the GS regime is not observed

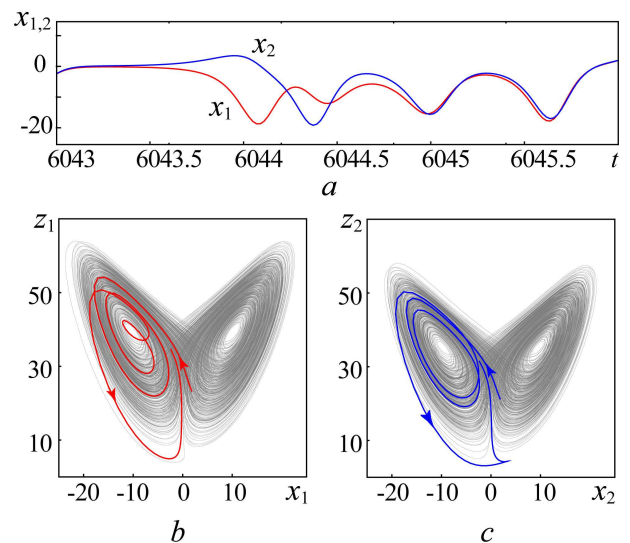


FIG. 6: (Color online) (*a*) The fragment of the time series of two mutually coupled Lorenz oscillators (13) corresponding to the short-term period of the phase trajectory divergence. (*b*) The phase portraits of Lorenz systems and the phase trajectories corresponding to the time interval shown in Fig. 6, *a*. The coupling strength $\varepsilon = 6.1$, the GS regime is detected

phase trajectory divergence that is responsible for the GS regime does not come into being. Above the critical point ε_{LE} there are also the phase trajectory divergencies, but they do not envelop both sheets of attractors and the representation points remain in the limits of one and the same sheet during this perturbations (Fig. 6).

The difference between these types of dynamics observed below and above the critical point ε_{LE} allows to explain the occurrence of the GS regime in two mutually coupled Lorenz systems (13). When the representation points are located at one and the same sheet of the chaotic attractor, the functional relation between vector states (2) is likely to exist, since the observed types of behavior is very close to the complete synchronization regime due to the rather large value of the coupling strength ε . Alternatively, the divergence of the phase trajectories on the different sheets of the chaotic attractor terminates this functional relation, and, in turn, the generalized synchronization regime is destroyed. So, below the critical point ε_{LE} the GS regime does not take place due to the presence of the short-term time intervals with the divergence of the phase trajectories on the different chaotic attractor sheets. More specifically, the intermittent behavior near the onset of the GS regime is observed (as well as in the vicinity of the other types of chaotic synchronization like lag synchronization [30, 31], phase synchronization [32, 33] and for generalized synchronization in the unidirectionally coupled oscillators [34]), that may be considered as the additional evidence of the correctness of the obtained results. Note, that above the onset of the GS regime (ε_{LE}) there are also the phase trajectory divergencies (which do not destroy the GS regime, since the representation points remain in the limits of one and the same attractor sheet and, as a consequence, the functional relation (2) takes place) preventing the occurrence of LS. These perturbations of the synchronous dynamics vanish above the critical point ε_{LS} where the lag synchronization regime comes into being.

So, having considered the behavior of two mutually coupled Lorenz system, we have obtained the additional evidence of the correctness of the proposed viewpoint on the GS regime in the systems with the mutual type of the coupling.

IV. GS IN NETWORKS OF COUPLED OSCILLATORS

Now we move to a more complicated situation, and analyze the GS in complex networks. As we have mentioned above, in this case between the interacting system states the functional relation in the form (3) should be established.

Developing the concept of GS in the mutually coupled oscillators for the networks, one can say that the phenomenon of GS in the complex network can be understood as the state of the whole network when the co-ordinates of all oscillators consisting this network are uniquely determined by the values of co-ordinates of only one node \mathbf{x}_k (chosen arbitrary). Following the arguments given in Sec. I, one can use for the generalized synchronization regime the implicit form of the functional relation between network's node states

$$\mathbf{x}_i(t^*) = \tilde{\mathbf{F}}[\mathbf{x}_k(t^*)], \quad \forall i \neq k, \quad (14)$$

where $t^* - \delta < t < t^* + \delta$ (where δ is infinitely small). Again, locally, in the given range $t^* - \delta < t < t^* + \delta$, we deal with the already known case. Under assumption $N_d = 3$ made above the following local Lyapunov exponents characterize the dynamics of the systems: $\lambda_1^k > 0$, $\lambda_2^k = 0$, $\lambda_3^k < 0$, $\lambda_{1,2,3}^i < 0 \quad \forall i \neq k$. In other words, in the selected area of the 3ND phase-space the manifold corresponding to the GS regime is characterized by one unstable direction \mathbf{e}^u and one direction with the neutral stability \mathbf{e}^0 lying inside this manifold, whereas all other directions are stable. These directions correspond to one positive, one zero and $(3N - 2)$ negative Lyapunov exponents. The same statement is also correct for the other moments of time t^* , therefore, for the complex network the manifold corresponding to the GS regime at every moment of time is characterized by one unstable direction, one direction with the neutral stability and $(3N - 2)$ stable directions. So, having calculated the spectrum of Lyapunov exponents for the network of coupled chaotic oscillators one obtain that the GS regime in this case produces one positive, one zero and $(3N - 2)$ negative Lyapunov exponents.

To prove the theoretical assumptions mentioned above we consider a network consisting of $N = 5$ Rössler systems with slightly mismatched ω -parameter values. The evolution of i -th node ($i = 1, \dots, N$) is described by the following equations

$$\begin{aligned} \dot{x}_i &= -\omega_i y_i - z_i + \varepsilon \sum_{j=1}^N G_{ij} x_j, \\ \dot{y}_i &= \omega_i x_i + a y_i, \\ \dot{z}_i &= p + z_i (x_i - c), \end{aligned} \quad (15)$$

where the values of the control parameters a , p , c have been chosen to be the same of the case of two coupled oscillators (8), $\omega_1 = 0.95$, $\omega_2 = 0.9525$, $\omega_3 = 0.955$, $\omega_4 = 0.9575$, $\omega_5 = 0.96$, $\mathbf{x}_i(t) = (x_i, y_i, z_i)^T$ is the vector-state of the i -th node, ε is the coupling strength between nodes, G_{ij} is the element of the coupling matrix \mathbf{G} . \mathbf{G} is a symmetric zero row sum matrix, with G_{ij} ($i \neq j$) being equal to 1 whenever node i is connected with node j and 0 otherwise, and $G_{ii} = -\sum_{j \neq i} G_{ij}$. The topology of the links between nodes in the network under study has been selected in such a way that each element of the network is connected with each other.

The dynamics of the considered network is characterized by $3N = 15$ Lyapunov exponents. If the coupling between nodes is equal to zero, there are N positive, N negative, and N zero Lyapunov exponents. With the increase of the coupling strength ε the zero Lyapunov exponents as well as the positive ones go gradually to the region of the negative values. The dependencies of the seven largest Lyapunov exponents on the coupling strength ε for the network consisting of five Rössler systems are shown in Fig. 7. One can see that at $\varepsilon_{LE} \approx 0.0385$ the second Lyapunov exponent λ_2 passes through zero and becomes negative. Therefore, the generalized synchronization regime is expected to be observed above the critical value ε_{LE} .

To prove the presence of GS we have used the nearest

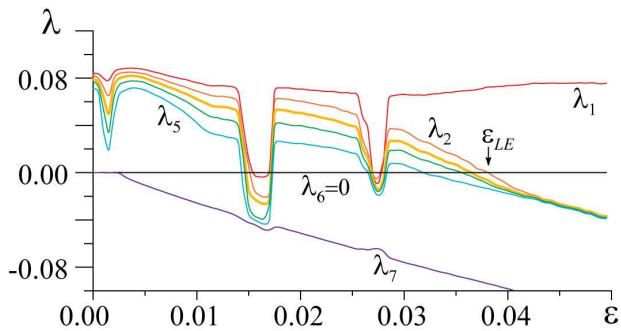


FIG. 7: (Color online) The dependencies of the seven largest Lyapunov exponents on the coupling strength ε for the network consisting of five Rössler systems (15). The onset of the GS regime in the network ε_{LE} is shown by the arrow

neighbor method in the same way as for two mutually coupled Rössler systems. In Fig. 8 the phase portraits of all Rössler systems of the network are shown for two values of the coupling strength, below (Fig. 8, *a*, $\varepsilon = 0.03$) and above (Fig. 8, *b*, $\varepsilon = 0.04$) the critical point ε_{LE} .

In the phase portraits of the three systems $\mathbf{x}_i(t)$, $i = 2 \div 4$ three points (one point for each system) with its nearest neighbors have been selected randomly (\blacklozenge — $i = 2$, $+$ — $i = 3$, \square — $i = 4$) and the points corresponding to them have been detected in all other coupled systems. For $\varepsilon = 0.03$ (Fig. 8, *a*) the points are concentrated in a limited range of attractor and distributed along the radius being the evidence of the presence of PS and the absence of GS. For $\varepsilon > \varepsilon_{LE}$ (Fig. 8, *b*) all states of all oscillators are nearest neighbors, thus proving the existence of GS.

Similarly to the case of two mutually coupled Rössler oscillators considered above we compare the onset of the GS and LS in the network (15). But due to the small values of the control parameter detuning the LS regime is very close to the complete synchronization (CS) one. In the simulations, the onset of the CS regime can be monitored by looking at the vanishing of the time average (over a window T) synchronization error

$$\langle E \rangle = \frac{1}{T(N-1)} \sum_{j>1} \int_t^{t+T} \|\mathbf{x}_j - \mathbf{x}_1\| dt'. \quad (16)$$

In the present case, we adopt as vector norm $\|\mathbf{x}\| = \sqrt{x^2 + y^2 + z^2}$. Fig. 9 reports the synchronization error versus ε for a given topology. One can see that the synchronization error becomes close to zero considerably later the GS regime arising. When the GS regime takes place $\langle E \rangle$ is still positive that is the evidence of the CS regime absence.

So, the GS regime in networks of coupled nonlinear elements can be detected by the moment of transition of the second (positive) Lyapunov exponent in the field of the negative values. Now we analyze the influence of the number of elements and topology of the network on the GS regime onset. In Fig. 10 the boundaries of the

GS regime on the “number of elements N — coupling parameter ε ”-plane for networks of different topologies of links between nodes are shown. Curve 1 corresponds to the random network whereas curves 2 and 3 refer to the regular and “small-world” networks, respectively. For all considered cases the values of the control parameters ω_i have been selected randomly in such a way that the probability distribution density of ω_i -values has been obeyed by the Gaussian distribution with the mean value $\omega_0 = 0.95$ and variance $\Delta\omega = 0.017$ that corresponds to the case of the relatively large values of the control parameter detuning. It is clearly seen from Fig. 10 that the topology of the network influences sufficiently on the GS regime onset. In particular, the threshold of the GS regime onset decreases for the random network, whereas both for the regular and “small world” ones it increases monotonically. At that, the boundary of GS for regular network grows more rapidly in comparison with the “small world” one.

V. MECHANISMS OF GS OCCURRENCE

Now, following the approach of some of our previous works [3], we move to reveal the mechanisms associated with the emergence of the GS regime in the case of a generic ensemble of coupled systems (with, obviously, the case of two coupled oscillators considered as the simplest variant of such a configuration).

For the purpose of exemplification, and without lack of generality, we here-below characterize the state of the network by the only vector $\mathbf{U} = (u_1, u_2, \dots, u_i, \dots, u_{N \cdot N_d})^T$, where $u_{3i-2} = x_i$, $u_{3i-1} = y_i$, $u_{3i} = z_i$, instead of the set of vectors $\mathbf{x}_i = (x_i, y_i, z_i)^T$, $i = 1, N$. The dimension of each element of the network is assumed to be $N_d = 3$ again, but this analytical study may be extended easily to the other systems with arbitrary dimensions N_d .

Following the above formalism, the entire network may be considered as a high-dimensional autonomous dynamical system, whose evolution equation is given by

$$\dot{\mathbf{U}} = \mathbf{L}(\mathbf{U}) + \varepsilon \tilde{\mathbf{G}}\mathbf{U}. \quad (17)$$

Here the vector function $\mathbf{L}(\cdot)$ determines the evolution of the elements of the network in the absence of the coupling, whereas the additive term $\varepsilon \tilde{\mathbf{G}}$ describes the influence of the topology and the coupling strength of the links between oscillators. Matrix $\tilde{\mathbf{G}}$ specifies the structure of the dissipative couplings between nodes, and it is assumed to be a symmetric zero row sum matrix, $\tilde{G}_{ii} = -\sum_{j \neq i} \tilde{G}_{ij}$, with \tilde{G}_{ij} ($i \neq j$) being equal to 1 whenever variable u_i forces the variable u_j and 0 otherwise.

It is easy to see that the term $\varepsilon \tilde{\mathbf{G}}\mathbf{U}$ brings the additional dissipation into the system (17). Indeed, the phase flow contraction is characterized by means of the vector

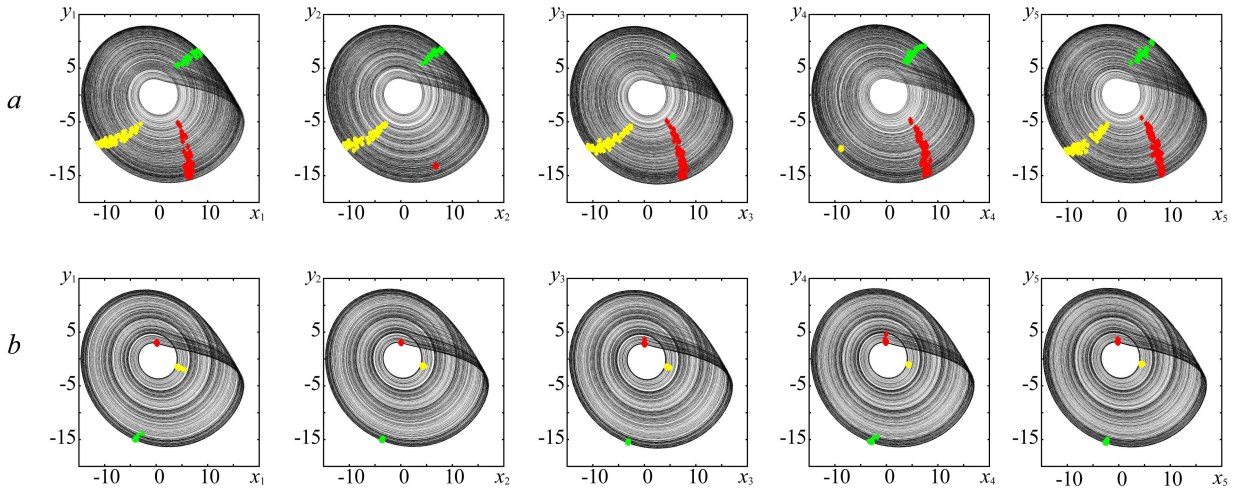


FIG. 8: (Color online) The phase portraits of five Rössler oscillators for two different values of the coupling parameter: (a) $\varepsilon = 0.03$ (the PS regime) and (b) $\varepsilon = 0.04$ (the GS regime)

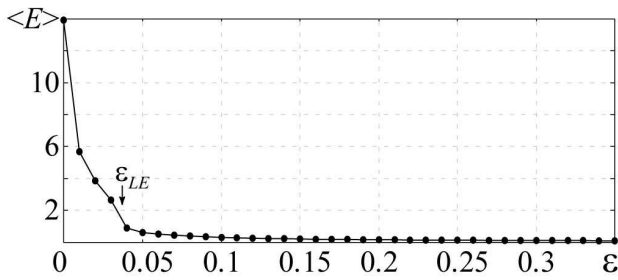


FIG. 9: $\langle E \rangle$ vs ε for the network of Rössler oscillators (15). The onset of the GS regime in the network ε_{LE} is shown by the arrow

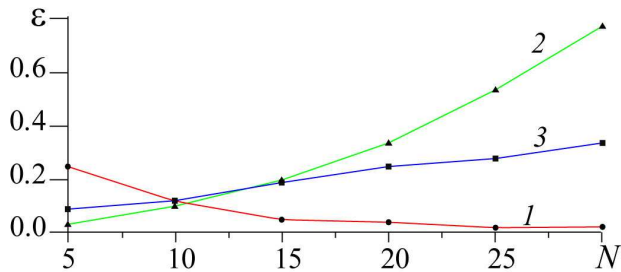


FIG. 10: (Color online) Boundaries of the GS regime on the “number of elements N — coupling parameter ε ”-plane for random (curve 1), regular (curve 2) and “small world” (curve 3) networks

field divergence

$$\lim_{\Delta t \rightarrow 0} \lim_{\Delta V \rightarrow 0} \frac{1}{\Delta V} \frac{\Delta V}{\Delta t} = \text{div } \mathbf{L} + \varepsilon \sum_{i=1}^{N_d N} \tilde{G}_{ii}, \quad (18)$$

where ΔV is the elementary volume of the phase space of the system (17). Since $\tilde{G}_{ii} \leq 0$, the term $\varepsilon \sum_{i=1}^{N_d N} \tilde{G}_{ii}$ is

also negative and the dissipation in the considered group increases with the growth of the coupling strength ε , resulting in the simplification of the otherwise chaotic dynamics of the system (17).

To characterize the complexity of the motion, the spectrum of Lyapunov exponents is frequently used. In the case under study, let’s suppose that the behavior of the system (17) is initially described by the set $\lambda_1 \geq \lambda_2 \geq \dots \geq \lambda_{N N_d}$ of Lyapunov exponents, with N of them being positive (i.e., while no synchronous motion is set up, each one of the elements of the network contributes independently with one positive Lyapunov exponent to the overall spectrum). As dissipation increases, some of the initially positive Lyapunov exponents become negative, and each passage of a Lyapunov exponent through zero testifies that one more degree of freedom of the chaotic motion corresponds to a contractive direction. When λ_2 becomes negative, only one degree of freedom is representative of the evolution of the network, i.e. a GS regime is built. Indeed, as soon as λ_2 is negative, all systems have to arrange their evolution into a specific collective motion, wherein the functional relation (3) is taking place.

CONCLUSION

In conclusion, we have analyzed the GS regime in systems with a mutual type of the coupling. We have extended the definition of GS, for being valid also for pairs of mutually coupled chaotic oscillators, and for the complex networks. The GS regime onset in 3D systems is shown to be connected with the zero-crossing of the second Lyapunov exponent. GS may be, therefore, considered in terms of the transition from the high-dimensional hyperchaotic regime to the chaotic oscillations. The obtained results are proved by means of the nearest neigh-

bor method. Since the developed theory is applicable to different systems, we expect that the very same mechanism will be observed in many other relevant circumstances. Particularly, the obtained results could be ex-

tended to the systems which dimension of the phase space $N_d > 3$ including the spatially extended media and coupled systems with a different dimension of the phase space.

-
- [1] S. Boccaletti, J. Kurths, G. V. Osipov, D. L. Valladares, and C. S. Zhou, *Physics Reports* **366**, 1 (2002).
- [2] H. D. I. Abarbanel, N. F. Rulkov, and M. M. Sushchik, *Phys. Rev. E* **53**, 4528 (1996).
- [3] A. E. Hramov and A. A. Koronovskii, *Phys. Rev. E* **71**, 067201 (2005).
- [4] L. Kocarev and U. Parlitz, *Phys. Rev. Lett.* **76**, 1816 (1996).
- [5] Z. Zheng and G. Hu, *Phys. Rev. E* **62**, 7882 (2000).
- [6] A. E. Hramov, A. A. Koronovskii, and P. V. Popov, *Phys. Rev. E* **72**, 037201 (2005).
- [7] N. F. Rulkov, *Chaos* **6**, 262 (1996).
- [8] E. A. Rogers, R. Kalra, R. D. Schroll, A. Uchida, D. P. Lathrop, and R. Roy, *Phys. Rev. Lett.* **93**, 084101 (2004).
- [9] B. S. Dmitriev, A. E. Hramov, A. A. Koronovskii, A. V. Starodubov, D. I. Trubetskov, and Y. D. Zharkov, *Physical Review Letters* **102**, 074101 (2009).
- [10] A. E. Hramov, A. A. Koronovskii, and P. V. Popov, *Phys. Rev. E* **77**, 036215 (2008).
- [11] J. Terry and G. VanWiggeren, *Chaos, Solitons and Fractals* **12**, 145 (2001).
- [12] A. A. Koronovskii, O. I. Moskalenko, and A. E. Hramov, *Physics-Uspokhi* **52**, 1213 (2009).
- [13] O. I. Moskalenko, A. A. Koronovskii, and A. E. Hramov, *Phys. Lett. A* **374**, 2925 (2010).
- [14] N. F. Rulkov, M. M. Sushchik, L. S. Tsimring, and H. D. I. Abarbanel, *Phys. Rev. E* **51**, 980 (1995).
- [15] L. M. Pecora and T. L. Carroll, *Phys. Rev. A* **44**, 2374 (1991).
- [16] K. Pyragas, *Phys. Rev. E* **56**, 5183 (1997).
- [17] K. Pyragas, *Phys. Rev. E* **54**, R4508 (1996).
- [18] *Encyclopaedia of Mathematics* (Springer-Verlag Berlin Heidelberg New York, 2002), Michiel Hazewinkel ed.
- [19] U. Parlitz, L. Junge, W. Lauterborn, and L. Kocarev, *Phys. Rev. E* **54**, 2115 (1996).
- [20] A. E. Hramov, A. A. Koronovskii, and O. I. Moskalenko, *Europhysics Letters* **72**, 901 (2005).
- [21] A. E. Hramov, A. A. Koronovskii, and M. K. Kurovskaya, *Phys. Rev. E* **75**, 036205 (2007).
- [22] A. E. Hramov, A. A. Koronovskii, and M. K. Kurovskaya, *Phys. Rev. E* **78**, 036212 (2008).
- [23] B. B. Godfrey, *Phys. Fluids* **30**, 1553 (1987).
- [24] H. Matsumoto, H. Yokoyama, and D. Summers, *Phys. Plasmas* **3**, 177 (1996).
- [25] D. I. Trubetskov and A. E. Hramov, *Lectures on microwave electronics for physicists* (Vol. 1,2. Fizmatlit, Moscow, 2003).
- [26] R. A. Filatov, A. E. Hramov, and A. A. Koronovskii, *Phys. Lett. A* **358**, 301 (2006).
- [27] A. Filatova, A. Hramov, A. Koronovskii, and S. Boccaletti, *Chaos: An Interdisciplinary Journal of Nonlinear Science* **18**, 023133 (pages 6) (2008).
- [28] P. J. Rouch, *Computational fluid dynamics* (Hermosa publishers, Albuquerque, 1976).
- [29] A. E. Hramov, A. A. Koronovskii, V. A. Maksimenko, and O. I. Moskalenko, *Physics of Plasmas* **19**, 082302 (2012).
- [30] S. Boccaletti and D. L. Valladares, *Phys. Rev. E* **62**, 7497 (2000).
- [31] M. Zhan, G. W. Wei, and C. H. Lai, *Phys. Rev. E* **65**, 036202 (2002).
- [32] S. Boccaletti, E. Allaria, R. Meucci, and F. T. Arecchi, *Phys. Rev. Lett.* **89**, 194101 (2002).
- [33] A. E. Hramov, A. A. Koronovskii, M. K. Kurovskaya, and S. Boccaletti, *Phys. Rev. Lett.* **97**, 114101 (2006).
- [34] A. E. Hramov and A. A. Koronovskii, *Europhysics Lett.* **70**, 169 (2005).
- [35] Except, may be, the finite number of points, which may be eliminated from the consideration without the lack of generality
- [36] E.g., this feature requires the proper choice of the reference point for the nearest neighbor method.